*Work supported by the National Science Foundation under Grant No. GP21311.

[1]L. P. Kadanoff, Physics 2, 263 (1966).
[2]L. P. Kadanoff *et al.*, Rev. Mod. Phys. 39, 395 (1967).
[3]G. Joyce, Phys. Rev. 146, 349 (1966).
[4]J. F. Nagle and J. C. Bonner, J. Phys. C 3, 352 (1970).
[5]See, for example, M. Kac, in *Brandeis Lectures*, 1966 (Gordon and Breach, New York, 1968); F. J. Dyson, Commun. Math. Phys. 12, 91 212 (1969); D. J. Thouless, Phys. Rev. 187, 732 (1969); P. W. Anderson, G. Yuval, and D. R. Hamaan, Phys. Rev. B 1, 4464 (1970).
[6]G. Stell, J. Chem. Phys. 51, 2037 (1969).
[7]G. Stell, Phys. Rev. Letters 24, 1345 (1970); Phys. Rev. B 2, 2811 (1970).
[8]G. Stell, in *Proceeding of the International School of Physics "Enrico Fermi," Course* 51 *on Critical Phenomena* (Academic, New York, to be published).
[9]N. S. Snider, J. Chem. Phys. 54, 4587 (1971).
[10]B. Widom, J. Chem. Phys. 43, 3892 (1965); 43, 3898 (1965).
[11]For example, M. Kac, G. E. Uhlenbeck, and P. C. Hemmer, J. Math Phys. 4, 216 (1963); P. C. Hemmer and G. Stell, Phys. Rev. Letters 24, 1284 (1970).
[12]G. Stell, Phys. Rev. 184, 135 (1969).
[13]W. K. Theumann, Phys. Rev. B 2, 1396 (1970).
[14]M. E. Fisher, Phys. Rev. 180, 594 (1969).
[15]M. J. Cooper, Phys. Rev. 168, 183 (1968). Using theorems of O. Penrose (unpublished) we have explored a "self-similarity" condition $G(\tilde{t},\tilde{h}) = \mathcal{G}[L, G(t,h)]$ which appears to be one of the few possibilities more general than (14) that can be naturally entertained within the context of the cell-function–site-function approach. This work will appear elsewhere. In connection with (1), it seems likely to us that such self-similarity will at the least prove relevant to certain borderline values of d/σ_m (such as those that appear in SM when $d/\sigma_m = 2$ and 1) at which logarithms occur.
[16]The content of footnote 40, Ref. 2, is that if one assumes (17a), one is forced to conclude that $\mathcal{L} \sim \langle s \rangle_L$, making it unnecessary to begin by postulating $\mathcal{L} \sim \langle s \rangle_L$. In strong scaling this demonstrates the redundancy of the postulate $\mathcal{L} \sim \langle s \rangle_L$. If one begins with the weak-scaling postulate that $f > 0$, as we do, it demonstrates instead the necessity of replacing (17a) by (17b).

PHYSICAL REVIEW B VOLUME 5, NUMBER 3 1 FEBRUARY 1972

Activation Volumes of Carbon Diffusion in fcc Iron-Nickel Alloys*

J. Keiser† and M. Wuttig
University of Missouri—Rolla, Rolla, Missouri 65401
(Received 20 August 1971)

The disaccommodation technique was used to determine the activation volume of carbon diffusion, ΔV, in six fcc iron-nickel alloys. Measurements were made at temperatures ranging from 68 to 90 °C and pressures up to 6 kbar on samples having a nickel content between 31 and 63 at.%. A maximum activation volume of 3.9 cm^3/mole was found at 34 at.% nickel. The compositional dependence of ΔV is satisfactorily reproduced by a magnetic-energy continuum model in which it is assumed that the activation free energy of diffusion is essentially ferromagnetic in origin.

I. INTRODUCTION

A thermally activated process is characterized by an activation free energy $\Delta\phi$. In the case of diffusion, $\Delta\phi$ is the free energy difference between the energy minimum and the saddle point in configurational space[1] of the crystal in which diffusion is occurring. The pressure derivative of the activation free energy is the activation volume ΔV. Physically, the activation volume of interstitial diffusion represents the change in volume of the crystal when a mole of interstitial atoms simultaneously moves from equilibrium sites to "activated sites."

In order to relate thermodynamic parameters of lattice defects such as the activation volume to the properties of the host crystal a continuum model may be used. In a continuum model the defect is viewed as a distortion of the continuum which displays the properties of the crystal being considered. For an estimate of the activation volume a strain-energy continuum model[2] has been used, in which the free energy of activation is assumed to be essentially a strain energy. On the basis of this assumption, the activation volume of diffusion was found to be

$$\Delta V_s = 2(\gamma - \tfrac{1}{3})\kappa\,\Delta\phi\ , \qquad (1)$$

where γ is the Grüneisen parameter and κ is the compressibility of the host lattice. Within the limitations of a continuum model, the activation volumes calculated from Eq. (1) agree with the experimental data except for carbon and nitrogen in iron,[2] which were also the only ferromagnetic systems examined. This apparent discrepancy inspired the investigation of the pressure dependence of the interstitial diffusivity in the nickel-carbon, cobalt-carbon, and iron-silicon-carbon systems, where it was also found that the strain-energy model did not estimate satisfactorily the experimentally de-

termined activation volumes.[3]

Since the systems displaying significant deviations from the estimates of the strain-energy model were all ferromagnetic, the assumption that the activation energy could be expressed as a strain energy was questioned and a magnetic contribution to $\Delta\phi$ was introduced. The resulting magnetic-energy continuum model is based on the assumption that the activation free energy represents the sum of the strain energy and the ferromagnetic exchange, anisotropy, and magnetoelastic energies. Upon neglecting the strain, anisotropy, and magnetoelastic energies, the activation volume of diffusion is found to be[3]

$$\Delta V_m = -\left[\sigma_0^{-1}\left(\frac{\partial\sigma_0}{\partial P}\right)_{H,T} + 2\kappa\right]\delta\,\Delta\phi\ , \qquad (2)$$

where σ_0 is the saturation magnetization per unit mass of the host lattice. The constant δ will be defined in Sec. IV. Experimentally determined values of the activation volumes of interstitial diffusion in ferromagnetic solids, ΔV_{expt}, and the estimates based on the strain-energy [Eq. (1)] and magnetic-energy [Eq. (2), $\delta = 1$] models are collected in Table I. None of the experimentally determined activation volumes is equal to either of the values ΔV_s or ΔV_m. As both ΔV_s and ΔV_m constitute limiting values it should not be expected that ΔV_{expt} agrees closely with either one. The inequality $\Delta V_m \leq \Delta V_{expt} \leq \Delta V_s$ is fulfilled, however.

From Eq. (2) it follows that if $\delta = 1$, the activation volume of diffusion in ferromagnetic solids should be controlled by the pressure dependence of the saturation magnetization. A systematic study of the influence of the pressure dependence of the saturation magnetization is afforded by the properties of the fcc iron-nickel alloys, as can be seen from the upper picture in Fig. 1.[7] The carbon diffusivity in this system is known[8] and its magnitude permits relaxation studies to be performed below the Curie temperature over a wide range of compositions, particularly in the Invar range of 30–40 at.% nickel. Therefore, the pressure dependence of the disaccommodation due to carbon diffusion in fcc iron-nickel alloys was measured and the results of this study will be reported in this paper.

TABLE I. Activation volumes of interstitial diffusion in ferromagnetic alloys.

Metal	Interstitial	θ/Θ[a]	ΔV_s	ΔV_m (cm^3/mole)	ΔV_{expt}
Fe	C	0.24	1.3	−0.7	0.037 ± 0.033[b]
		0.24			0.0 ± 0.1[c]
	N	0.23	1.2	−0.6	−0.040 ± 0.035[d]
Fe-Si	C(1)	0.25	1.3	−0.7	0.3 ± 0.3[e]
	(Fe-C-Fe) C(2) (Fe-C-Si)	0.25	1.3	−0.7	−0.6 ± 0.9[e]
hcp Co	C(1)	0.25	1.7	−0.8	−1.7 ± 2.0[e]
	C(2)	0.25	1.6	−0.8	−0.5 ± 0.2[e]
Ni	C	0.61	2.5	−1.4	1.2 ± 0.1[e]

[a] θ is the measuring temperature. Θ is the Curie temperature.

[b] Reference 4.

[c] Reference 5.

[d] Reference 6.

[e] Reference 3.

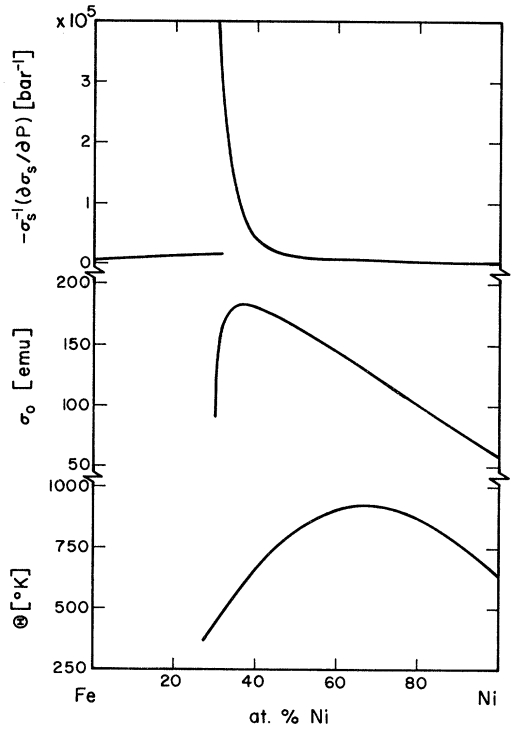

FIG. 1. Selected ferromagnetic properties of iron-nickel alloys (Ref. 7). The saturation magnetization at room temperature is denoted by σ_s and at 0 °K by σ_0.

II. EXPERIMENTAL PROCEDURE

A. Sample Preparation

Iron-nickel samples were prepared by sintering and were subsequently carburized in a conventional manner. For the sintering process, appropriate amounts of nominally 99.999% Johnson, Matthey, and Company nickel sponge and 99.999% United Mineral and Chemical Company iron sponge were carefully mixed followed by sintering in dry H_2 for 8 h at temperatures about 20 °C below the solidus temperature. After sintering, the samples were swaged and recrystallized in vacuum at 1200 °C. The carburization was performed by packing the samples in powdered reactor-grade graphite and annealing in 500 μ of air for appropriate times at temperatures chosen to give a carbon content of

TABLE II. Compositions of samples.

at. % Ni		
Nominal	Actual	at. % C
63	62.88	0.87
39	39.44	0.98
36	36.08	0.90
34	33.72	0.90
31a	31.43	0.82
31b	31.45	0.85

0.9 at. % (± 10%). Following carburization, the samples were homogenized at 1200 °C in vacuum and subsequently water quenched. The carbon content was determined by weighing and the nickel content by chemical analysis. The compositions of the six samples investigated are given in Table II.

B. Experimental Apparatus

The experimental apparatus consisted of a disaccommodation-measuring system and an environment-control system with which the pressure and temperature could be selected.

The pressure system consisted of two high-pressure vessels and a commercially available pumping system. The smaller pressure vessel contained the manganin coil used to determine the pressure. Because the resistivity of the manganin is a (weak) function of temperature, the pressure vessel was kept in a constant temperature bath at (31 ± 1) °C. The larger pressure vessel housed the solenoid used for the disaccommodation measurements. This pressure apparatus was capable of maintaining the pressure constant to ± 10 bar and the temperature control system could maintain the temperature of the larger vessel to ± 0.04 °C; it was the same as that used for previous disaccommodation measurements,[3] except for the following improvements.

The high-pressure vessels and plugs were made of 18% nickel, 300 000-psi yield strength Mar-Aging steel to extend the pressure and temperature operating ranges.

The sheathed electrical feedthroughs[9] were vacuum brazed to a Bridgman-type stainless-steel cone, and the cone was held against the plug with a special nut to form a pressure-tight metal-on-metal seal. To prevent oil leakage through the ceramic insulation of the sheathed wires, the ends of the wires were protected by a layer of General Electric silicon seal.

A triangular cross-section stainless-steel anti-extrusion ring was incorporated into the seal for the high-pressure plug.

C. Measurements

The disaccommodation technique[10] was used to determine the pressure dependence of the carbon diffusivity. This technique yielded directly the relaxation time of carbon redistribution with respect to the spontaneous magnetization. If the elementary diffusive jump of the redistribution mode giving rise to the disaccommodation is the same as that responsible for long-range diffusion, this relaxation time is inversely proportional to the diffusivity.[11]

The actual experimental work consisted of measuring the exponential decrease in the initial permeability of the demagnetized samples at pressures from ambient to 6 kbar. The automatic bridge used to make the disaccommodation measurements has been described previously.[12] The reciprocal of the permeability, the reluctivity ν, was normalized and fitted by a least-squares analysis[13] to one or a sum-of-two independent exponentials. In the analysis, equal weight was given to each data point. These calculations yielded the relaxation amplitude, the relaxation time τ, and the half-width β of the Gaussian distribution of the relaxation time.

The measuring temperatures ranged from 68 to 90 °C. They were chosen so that the initial portions of the disaccommodation could be measured reliably and such that the runs did not last more than 18 h over which period the environmental parameters stayed within the above specifications. All runs were terminated when the disaccommodation had decreased to 0.1% of its initial value. The maximum temperature variation between runs of any one alloy at various pressures was 0.20 °C. The relaxation times were corrected for these small temperature variations using the known activation energies of carbon diffusion in iron-nickel alloys.[8]

III. RESULTS

The experimental data were analyzed both in terms of a single relaxation and in terms of a sum-of-two independent relaxations. Figure 2 shows some representative data points obtained for the 34% nickel 6-kbar run on a plot of normalized reluctivity vs the logarithm of the normalized time.[13] Included in Fig. 2 are two calculated curves which describe the disaccommodation in terms of one relaxation and in terms of two relaxations. It can be seen from this figure that the two-relaxation analysis describes the data better than the one-relaxation analysis does. This was the case for all data taken.

The analysis of each set of data in terms of two relaxations gave two sets of amplitudes, relaxation times, and half-widths. For all alloys it was found that the short-time relaxation accounted for a large percentage (59–76%) of the total amplitude. Therefore, all further mention of experimental results refers to the results for the short-time large-amplitude relaxation. It should be noted that all three sets of calculated relaxation times satisfy the con-

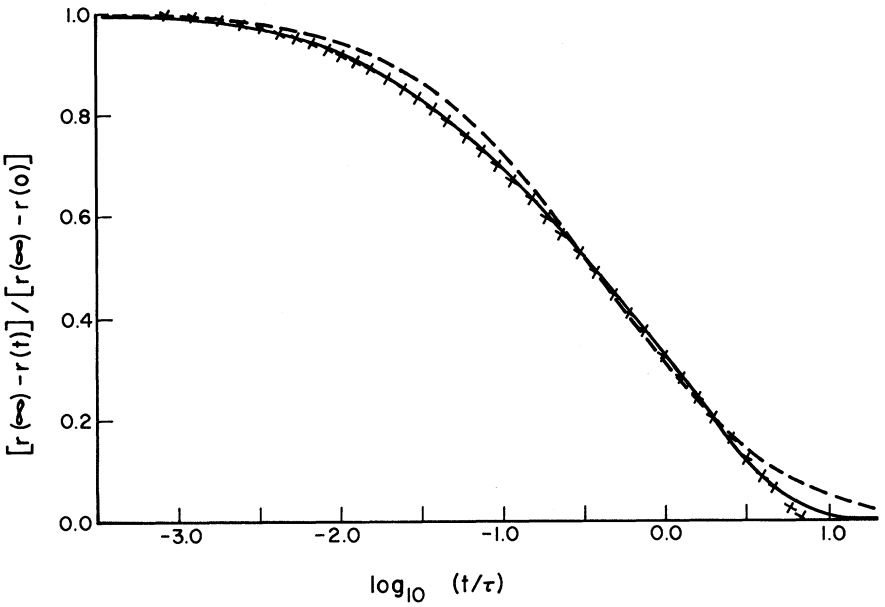

FIG. 2. Normalized reluctivity as a function of the logarithm of the normalized time of a 34 at.% nickel alloy at 6 kbar. Representative data points are indicated by X's and the results of a least-squares analysis in terms of one (dashed line) and two (straight line) relaxations are shown.

clusion of this work.

The relaxation time of carbon redistribution of all alloys increased with pressure. Figure 3 shows the logarithm of the normalized relaxation time vs pressure for the six alloys examined. The straight lines are the results of a linear least-squares fit used to calculate the activation volume according to[14]

$$\Delta V = RT\left(\frac{\partial \ln \tau}{\partial P}\right) . \tag{3}$$

All activation volumes of carbon diffusion in the six iron-nickel alloys resulting from these calculations (ΔV_{expt}) are plotted in Fig. 4. The error limits represent the values obtained from the linear least-squares fit to the data plotted in Fig. 3. Some of them are unexpectedly large; a fact which will be commented on in Sec. IV.

No significant variation of the half-width as a function of pressure or composition was detected.

The total relaxation amplitude was a function of composition and it followed as it should the experimental results for the carbon-induced crystal anisotropy energy[15,16] in iron-nickel alloys.[8]

Unlike the compositional dependence of the amplitude, the pressure dependence of the amplitude displayed no readily discernible pattern.

IV. DISCUSSION

In the Introduction it was stated that a continuum model for solids was used to develop the expressions for the activation volume. In a continuum model the defect properties are assumed to be determined by the properties of the host solid. Therefore, the type of defect is not critical, although it must be expected that a continuum model is more valid the smaller the defect concentration and the less complex the nature of the defects. The results of the least-squares analysis are that two relaxations describe the data better than one relaxation,

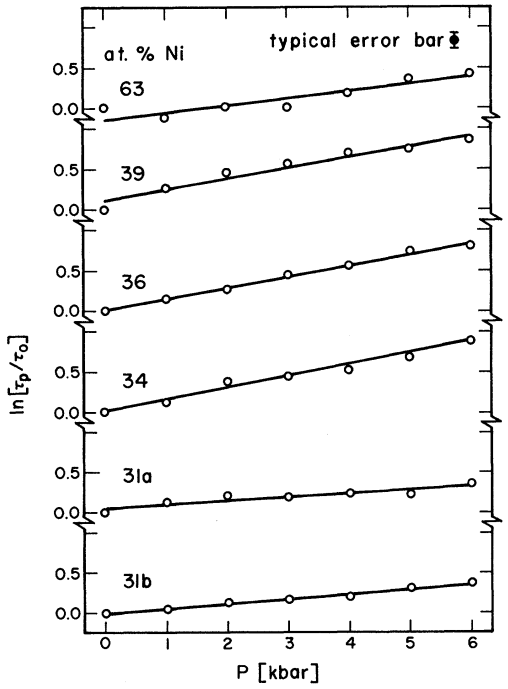

FIG. 3. Pressure dependence of the relaxation time of carbon diffusion in six iron-nickel alloys. τ_p is the relaxation time at pressure p; τ_0 is the relaxation time at ambient pressure.

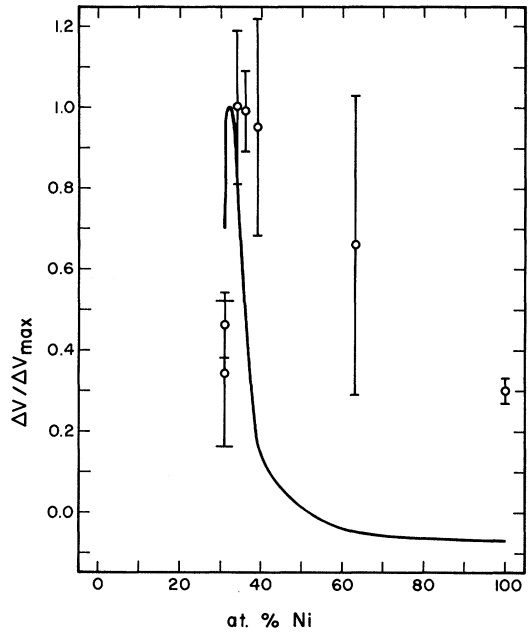

FIG. 4. Normalized activation volume of carbon diffusion in fcc iron-nickel alloys. The solid line shows the activation volume calculated from Eq. (4). The data points are from Table III. The experimental activation volume for pure nickel was taken from Ref. 3.

and this may be interpreted to mean that either more than one defect species contributes to the total disaccommodation or that the redistributing defect is characterized by more than one time constant.[17] It is thought that the main contribution to the observed disaccommodation is due to single interstitials,[8] which would indicate that the activation volumes ΔV_{expt} represent activation volumes of diffusion. The present carbon concentration of 0.9 at.% was chosen because it gives an average carbon separation of about three fcc lattice parameters. If single interstitial atoms are indeed responsible for the disaccommodation the three-cell spacing between carbon atoms should minimize the effects of carbon-carbon interactions and render the magnetic continuum model more realistic.

From the equation for the magnetic-energy continuum model [Eq. (2)] it can be seen that the activation volume ΔV_m is proportional to $\sigma_0^{-1}(\partial\sigma_0/\partial P)_{H,T}$. As shown in the upper part of Fig. 1, this factor increases very rapidly as the nickel content is reduced to 30 at.%, so ΔV_m will also show a rapid increase in the same composition range. However, the experimentally determined activation volumes given in Table III display a maximum at 34 at.% nickel, so the agreement between ΔV_m and ΔV_{expt} is poor. An improvement of the theoretical estimates can be based on a reexamination of the term $\Delta\phi$ in Eq. (2). Within the confines of the magnetic-energy continuum model the free energy $\Delta\phi$ is proportional to the saturation magnetization. Consequently, $\Delta\phi$ should exhibit the same variation with temperature as σ does. Since $\sigma_\theta \simeq \sigma_0$ for $\theta/\Theta < 0.6$ (θ is the measuring temperature and Θ is the Curie temperature) it can be seen from Table I that the previous results did not need to be corrected for the effects of the temperature on σ. For some of the alloys investigated in this study, however, the measuring temperature approaches the Curie temperature, as can be seen in Fig. 1 and Table III. Therefore, the correction factor σ_θ/σ_0 must be included in Eq. (2) in order to account for the fact that the ratio θ/Θ is not smaller than 0.6.

Besides being a function of temperature, the saturation magnetization of the nickel-iron base alloys is also a function of composition, as shown in Fig. 1. Therefore, a second correction is needed to account for this fact. This correction should be σ_a/σ_{r0}, where σ_a is the saturation magnetization of the alloy being considered and σ_{r0} is the saturation magnetization at 0 °K of a reference alloy. For the calculations leading to the results shown in Fig. 4, the 36 at.% nickel alloy was used as a reference.

It follows that $\delta = \sigma_\theta\,\sigma_a/\sigma_0\,\sigma_{r0}$ and the activation volume of diffusion in the iron-nickel system is

$$\Delta V_m \propto \left[\sigma_0^{-1}\left(\frac{\partial\sigma_0}{\partial P}\right)_{H,T} + 2K\right]\frac{\sigma_\theta\,\sigma_a}{\sigma_0\,\sigma_{r0}} \quad . \tag{4}$$

As can be seen from Fig. 4, this expression and therefore the magnetic-energy model predicts the position of the maximum found in the experimentally determined activation volumes ΔV_{expt} and reproduces the compositional dependence of ΔV_{expt} when $\sigma_0^{-1}(\partial\sigma_0/\partial P)_{H,T}$ is large. When $\sigma_0^{-1}(\partial\sigma_0/\partial P)_{H,T}$ is small, the model less satisfactorily reproduces the compositional dependence. Extension of the model to include one or more of the neglected energy terms might result in a better description of the experimental results, but a lack of experimental data, especially for the magnetostriction, makes an extension of the model unwarranted.

Consequently, the results of this study lend support to the idea that in calculating the diffusion parameters of ferromagnetic solids the exchange

TABLE III. Experimental results.

Nominal at.% Ni	ΔV_{expt} (cm³/mole)	θ/Θ
63	2.59 ± 1.47	0.40
39	3.74 ± 1.07	0.52
36	3.90 ± 0.38	0.63
34	3.94 ± 0.76	0.66
31a	1.35 ± 0.70	0.89
31b	1.81 ± 0.33	0.90

interaction cannot be ignored.

A final comment concerns the undesirably large error limits of the values ΔV_{expt} listed in Table III and shown in Fig. 4. A hint of an explanation is contained in Fig. 3, where it can be seen that the deviations of the data points from the least-squares line are nonrandom. Physically, this phenomenon may be a consequence of the fact that the activated state changes its position in configurational space as a function of pressure, i.e., when the interatomic spacing is changed. In iron-nickel alloys with their competing ferromagnetic and antiferromagnetic interactions[18] this is possible. Thus, the large error limits of ΔV_{expt} may merely reflect the force fitting of the data which was prompted by the simple model used to interpret the data.

ACKNOWLEDGMENT

The authors wish to thank Al Baisch, Designs for Tomorrow, Inc., for his cooperation in the manufacture of the high-pressure hardware.

*Work supported by the National Science Foundation under Grant No. NSF GK-18460. It also benefitted from the support of the American Iron and Steel Institute.

†Submitted in partial fulfillment of the requirements of the degree Ph.D. in Metallurgical Engineering.

[1]George H. Vineyard, J. Phys. Chem. Solids 3, 121 (1957).

[2]R. W. Keyes, in *Solids Under Pressure*, edited by W. Paul and D. M. Warschauer (McGraw-Hill, New York, 1963).

[3]M. Wuttig and J. Keiser, Phys. Rev. B 3, 815 (1971).

[4]A. J. Bosman, P. E. Brommer, L. C. H. Eijkelenboom, C. J. Schinkel, and G. W. Rathenau, Physica 26, 533 (1960).

[5]J. Bass and D. Lazarus, J. Phys. Chem. Solids 23, 1820 (1962).

[6]A. J. Bosman, P. E. Brommer, and G. W. Rathenau, Physica 23, 1001 (1957).

[7]J. S. Kouvel and R. H. Wilson, J. Appl. Phys. 32, 435 (1961).

[8]E. Adler and C. Radeloff, J. Appl. Phys. 40, 1526 (1969).

[9]W. Paul, G. B. Benedek, and D. M. Warschauer, Rev. Sci. Instr. 30, 874 (1959).

[10]S. Chikazumi, *Physics of Magnetism* (Wiley, New York, 1964).

[11]C. Wert and C. Zener, Phys. Rev. 76, 1169 (1949).

[12]M. Wuttig and H. K. Birnbaum, J. Phys. Chem. Solids 27, 225 (1966).

[13]J. R. Keiser and M. Wuttig, Acta Met. 19, 445 (1971).

[14]D. Lazarus and N. H. Nachtrieb, in Ref. 2.

[15]D. Polder, Phillips Res. Rept. 1, 5 (1945).

[16]L. Néel, J. Phys. Radium 13, 249 (1952).

[17]A. S. Nowick, Advan. Phys. 16, 1 (1967).

[18]E. Adler and C. Radeloff, Z. Angew. Phys. 26, 105 (1969).

PHYSICAL REVIEW B VOLUME 5, NUMBER 3 1 FEBRUARY 1972

Domain and Wall Hyperfine Fields in Ferromagnetic Iron

M. A. Butler, G. K. Wertheim, and D. N. E. Buchanan
Bell Telephone Laboratories, Murray Hill, New Jersey 07974

(Received 12 August 1971)

The Mössbauer effect and nuclear magnetic resonance are used to examine the temperature dependence of the domain and wall hyperfine fields in ferromagnetic iron. The difference between them is attributed to demagnetizing fields and exhibits a temperature dependence different than predicted from consideration of domain and wall spin-wave excitations. It is proposed that this temperature dependence arises from distortion of domain shapes with temperature. After correction to constant volume, the temperature dependence of the hyperfine field is compared with that of new magnetization measurements. It is shown that an intrinsic temperature dependence of the effective hyperfine coupling constant exists and may be qualitatively explained by three mechanisms: (i) phonon admixture of the s and d wave functions, (ii) Stoner-like excitations combined with a strongly energy-dependent hyperfine coupling constant, and (iii) changes in the intrinsic s-d hybridization due to the changing magnetization. It is concluded that differentiation of the three mechanisms is not possible by the present type of experiment but requires reliable theoretical estimates of the magnitudes of the various effects.

I. INTRODUCTION

While techniques for measuring hyperfine fields have long been used to study the ferromagnetic metals, the interpretation of the dependence of hyperfine fields on thermodynamic variables and the relation of such fields to the bulk magnetization is complicated by numerous factors: (i) Most experiments are performed at constant pressure, so that the data must be corrected to constant volume